
Article:
Borràs-Gas, H., Solé-Soler, R., do Aido-Machado, R. et al. (2026) Molecular basis for the regulation of the SUMOylation activity of the Smc5/6 complex by Esc2. Communications Biology. ISSN: 2399-3642

https://doi.org/10.1038/s42003-026-10806-8

---

communications biology

A Nature Portfolio journal

Article

Article in Press

https://doi.org/10.1038/s42003-026-10806-8

Molecular basis for the regulation of the SUMOylation activity of the Smc5/6 complex by Esc2

Helena Borràs-Gas[1], Roger Solé-Soler[2], Rodolpho do Aido-Machado[3], Martina Matas[1], Michael P. Williamson[3], Nathalia Varejão[1] ✉, Jordi Torres-Rosell[2] & David Reverter[1] ✉

Post-translational modification by SUMO regulates a wide array of cellular processes. Despite the large number of SUMOylated substrates, only a limited set of SUMO E3 ligases have been identified, raising important questions about how substrate specificity is achieved. In budding yeast, the nuclear protein Esc2 functions as a cofactor in the SUMO pathway through its interaction with the E2 enzyme Ubc9. Esc2 is relevant under conditions of replicative stress, promoting the removal of recombination intermediates during DNA replication. This role has been largely attributed to its ability to enhance the SUMO E3 ligase activity of Nse2, a subunit of the Smc5/6 complex. Here, we uncover the molecular mechanism underlying Esc2-mediated stimulation of Nse2-dependent SUMOylation by identifying a direct interaction between the C-terminal SUMO-interacting motif of Nse2 and the Esc2 SLD2 domain. These coordinated interactions facilitate the formation of a productive E3-E2~SUMO complex and promote efficient SUMO transfer to substrates such as Sgs1 and Top3, thereby enhancing the processing of recombination intermediates and contributing to genome integrity.

SUMOylation is a post-translational protein modification that regulates multiple functions within the cell, including nuclear transport, gene expression, or DNA damage response, among others[1–4]. SUMO (Small Ubiquitin-like Modifier), like ubiquitin, is conjugated via its C-terminal tail through a multi-step enzymatic cascade, including E1 activation, E2 conjugation, and E3 ligation, forming an isopeptidic bond to lysine residues of target proteins[5,6]. SUMOylation typically modulates protein-protein interactions by binding to specific SUMO interaction motifs (SIMs) in substrates[7–9]. SUMO modification is ubiquitous across eukaryotes. Human cells contain four SUMO isoforms (SUMO1, SUMO2, SUMO3, and SUMO4), plants have multiple, but most invertebrates and yeast have only one (Smt3 in budding yeast)[10,11].

During the SUMOylation pathway, the E1 activating enzyme transfers a thioester-bound SUMO to a cysteine residue of the E2, forming the E2~SUMO thioester (transient thioester bond between E2 and SUMO), which is ultimately discharged on a lysine residue of the substrate[5,6]. However, this E2~SUMO thioester discharge can be stimulated by E3 ligases, facilitating substrate binding and enhancing the isopeptide linkage to a substrate lysine. The SUMO E3 ligase stabilizes a fixed active conformation of the E2~SUMO thioester, thus reducing its conformational freedom[5]. While the ubiquitin conjugation pathway contains a large number of encoded E3 ligases, only a few bona fide E3 ligases have been discovered for SUMO[6]. *Saccharomyces cerevisiae* contains three mitotic SUMO E3 ligases: Siz1, Siz2 (PIAS in humans), and Nse2 (or Mms21), which bind the charged E2 by means of their conserved SP-RING domain[12,13]. However, structures of E2-E3 complexes revealed the presence of additional interfaces containing SIM motifs to enhance the E2~SUMO discharge reaction[7], such as an extra SIM stabilizing a second SUMO bound to the E2 backside during the E3-dependent reaction[13,14]. This non-covalent binding to the E2 backside has been reported to increase the rate of SUMO or ubiquitin chain formation[7,15,16].

Enhancer of Silent Chromatin 2 (Esc2) is a conserved nuclear protein from *Saccharomyces cerevisiae* that plays a multifaceted role in genome maintenance. It is characterized by the presence of two SUMO-like domains (SLDs). Esc2 is a member of the so-called RENi-family (RENi is short for Rad60-Esc2-NIP45)[17]. By this name, the other ortholog proteins sharing the presence of SUMO-like domains were classified, being Rad60 in *S. pombe* and Nip45 (NFAT Interacting Protein 45) in humans. Esc2 has been implicated in processes such as DNA replication, recombination, and transcriptional silencing, and it is particularly relevant under conditions of replication stress[18–21]. Although it lacks enzymatic activity, Esc2 seems to

[1]Institut de Biotecnologia i Biomedicina and Departament de Bioquímica i Biologia Molecular. Universitat Autònoma de, Barcelona, Spain. [2]IRBLLEIDA, Dept. Ciències Mèdiques Bàsiques, Universitat de Lleida, Lleida, Spain. [3]School of Biosciences, The University of Sheffield, Sheffield, UK.
✉e-mail: nathalia.varejao@uab.cat; david.reverter@uab.cat

function as a regulatory scaffold, coordinating protein-protein interactions[22].

An intriguing aspect of Esc2 is its involvement in the SUMOylation pathway, in particular, the SLD2 domain of the RENi members is able to bind the backside of the SUMO E2 (Ubc9) and potentially act as a cofactor during the SUMO conjugation reaction[17,22–24]. Although Esc2 lacks a canonical SUMO E3 ligase domain, it has been proposed to facilitate SUMO transfer by stabilizing the interaction between Ubc9 and specific substrates[24]. This pseudo-E3 activity may be particularly relevant under conditions of replicative stress, where SUMOylation of DNA repair proteins is critical[1,25]. In particular, Esc2 has been shown to facilitate the SUMOylation conducted by Nse2/Mms21, a subunit of the Smc5/6 complex with SUMO E3 ligase activity[24,26].

The Smc5/6 complex is crucial for resolving recombination structures and maintaining replication fork stability, and Esc2 appears to enhance these functions by coordinating recombination-associated repair pathways. Genetic studies show that the absence of Esc2 or the Smc5/6 complex leads to the accumulation of recombination intermediates and to genome instability[18]. In particular, it has been reported in yeast that the Smc5/6 complex SUMOylates the STR complex (Sgs1-Top3-Rmi1 complex), involved in the dissolution of Holiday Junction (HJ) structures to proceed with DNA repair processes by homologous recombination (HR)[27–29], an activity stimulated by the presence of Esc2[21,24,29]. However, the molecular mechanism by which Esc2 modulates SUMOylation activity of the Smc5/6 complex remains to be fully elucidated.

In this study, we demonstrate that Esc2 enhances the SUMOylation activity of the Smc5/6 complex during the catalytic reaction by simultaneously binding to the backside of Ubc9 and the SIM2 motif located at the C-terminus of Nse2. Based on these findings, we propose that the SLD2 domain of Esc2 functions as a positive cofactor of the Smc5/6 catalyzed conjugation reaction, promoting E2-mediated SUMO transfer to substrates. This effect likely arises from its ability to mimic the non-covalent interaction between SUMO and Ubc9 that typically occurs during E3-catalyzed reactions.

Results

Esc2 SLD2 domain binds the C-terminal Nse2 SIM2

A major feature of the three RENi family members, Rad60, Nip45, and Esc2, is the presence of two SUMO-like globular domains connected by disordered regions of varying lengths. Each SUMO-like domain (SLD) of Esc2 possesses different homologies compared to Smt3 (the yeast SUMO protein), SLD2 being more similar to SUMO with a RMSD value (root mean square deviation) of 1.22 Å with 17% of sequence identity, in contrast to 1.54 Å and 9% of sequence identity for SLD1 (Fig. 1a, b). The sequence identity of the disordered segments in the RENi family is poorly conserved compared to the SLD domains (Supplementary Fig. 1), and these regions also vary in length, as observed in the AlphaFold3 models of the three RENi members (Supplementary Fig. 2). Our initial attempts to express full-length Esc2 in *E. coli* were unsuccessful. However, we could produce three Esc2 truncated constructs: $Esc2_{146\text{-}456}$, which includes the putative N-terminal DNA-binding domain along with SLD1 and SLD2; $Esc2_{191\text{-}456}$, containing the SLD1 and SLD2 domains; and $Esc2_{374\text{-}456}$, containing only the SLD2 domain (Supplementary Fig. 3).

To assess whether the Esc2 SLD2 domain directly binds the C-terminal SIM motif of Nse2 in a manner similar to Smt3, which can simultaneously engage the backside of Ubc9 and the Nse2 SIM2 (Fig. 1c, d), we performed an NMR titration experiment using a synthetic 13-residue peptide corresponding to the C-terminus of Nse2. The 13-mer SIM-containing peptide was titrated into the $Esc2_{374\text{-}456}$ WT sample at increasing molar ratios (1:0.5; 1:1; 1:2; 1:4). At each addition, a 2D ^{1}H–^{15}N HSQC spectrum was acquired to monitor Chemical Shift Perturbations (CSP). Upon addition of SIM-containing peptide into $Esc2_{374\text{-}456}$ WT the CSP observed were small but specific, suggesting direct binding between the protein and the peptide with low affinity, also represented by the fast exchange regime (Fig. 1e)[30–32]. The 20 residues with the largest CSP were fitted simultaneously, giving an estimated K_D value of 900 μM, which agrees with the magnitude of the observed CSPs. An AlphaFold model of the Nse2 SIM2 bound to the Esc2 SLD2 domain suggests an interaction mode similar to that observed in the Smt3 complex structure[13] (Fig. 1f).

Esc2 does not function as a SUMO E3 ligase

It has been reported that the SLD2 domain of Esc2, like those of the other RENi family members Nip45 and Rad60, binds to the backside surface of Ubc9, the SUMO E2-conjugating enzyme[21,22,33] (Fig. 1). Thus, because these proteins interact with the SUMO E2-conjugating enzyme, RENi family members have been proposed to function as SUMO E3 ligases that enhance SUMOylation of DNA repair factors, including the targeting of SLX4 during the resolution of double-stranded DNA catenates in M phase[23].

Using two Esc2 truncation constructs, $Esc2_{146\text{-}456}$, and $Esc2_{374\text{-}456}$, we performed in vitro single-turnover assays to monitor the transfer of SUMO from the E2~SUMO thioester to a substrate lysine within the C-terminal region of p53 and resulting in the formation of an isopeptide bond (Fig. 2). A defining characteristic of bona fide E3 ligases, particularly in the SUMOylation pathway, is their ability to enhance SUMO discharge from E2 to the substrate. To specifically track this activity within the SUMO cascade, we utilized a fluorogenic SUMO mutant, D68R Smt3. This variant can be activated by the SUMO E1 enzyme similarly to the wild-type Smt3, but notably, it lacks binding affinity for the E2 backside, allowing for selective monitoring of E3-dependent SUMO transfer[34,35].

As expected, Nse2/Arm-Smc5 E3 ligase stimulated discharge of the E2~Smt3 thioester onto the substrate under stoichiometric conditions, as observed by the depletion of the Ubc9~Smt3 and the concomitant appearance of the cp53-Smt3 conjugate over time (Fig. 2a). In contrast, both Esc2 SLD1–SLD2 tandem construct and the isolated SLD2 domain failed to increase the E2~SUMO thioester discharge in the absence of the E3 ligase (Fig. 2a). To further investigate the potential SUMO E3 ligase activity of yeast Esc2, similar single-turnover assays were conducted in the absence of an external acceptor substrate monitoring the depletion of the E2~SUMO thioester. Consistent with the results above, neither Esc2 construct promote enhanced discharge of the E2~SUMO thioester, whereas Nse2/Arm-Smc5 markedly accelerated discharge under the same conditions (Fig. 2b). While we cannot rule out the possibility that Esc2 may require specific cofactors or cellular conditions to exhibit E3 ligase activity, our in vitro data indicates that Esc2 does not function as a SUMO E3 ligase under the tested conditions.

These findings indicate that Esc2 does not independently facilitate SUMO transfer to substrates in the manner expected for a canonical SUMO E3 ligase. According to the textbook definition, a SUMO E3 ligase is a protein that promotes and enhances SUMO conjugation by stabilizing the interaction between E2 and the substrate. Based on this criterion, Esc2 does not fulfill the role of a SUMO E3 ligase. However, when both Nse2/Arm-Smc5 (an established SUMO E3 ligase) and Esc2 constructs are present in the same reaction, the efficiency of SUMO transfer is significantly increased under all conditions tested (Fig. 2).

SLD2 of Esc2 enhances Nse2-mediated SUMOylation

Despite Esc2 lacking intrinsic SUMO E3 activity, we observed that it can enhance Nse2/Arm-Smc5, potentially by acting as a SUMO E2 cofactor that interacts with the backside of the SUMO-conjugating enzyme Ubc9 (Fig. 2)[24,26]. Structural superposition of the AlphaFold3 model of Esc2 SLD2 with Smt3 (yeast SUMO) suggests that SLD2 may mimic a SUMO molecule that can bind to the E2 backside, thereby potentially enhancing SUMO discharge onto substrates (Fig. 1). This resemblance raises the possibility that Esc2 SLD2 functions as a positive allosteric modulator of Nse2/Arm-Smc5's E3 ligase activity, facilitating more efficient SUMO transfer. For instance, the key SUMO residues involved in interactions with the E2 enzyme's backside and with the SIM2 motif of Nse2 are largely conserved within the SLD2 (Fig. 1a, red colored).

To test this hypothesis, we performed single-turnover assays using the D68R-Smt3~Ubc9 thioester comparing the effects of additional unlabeled

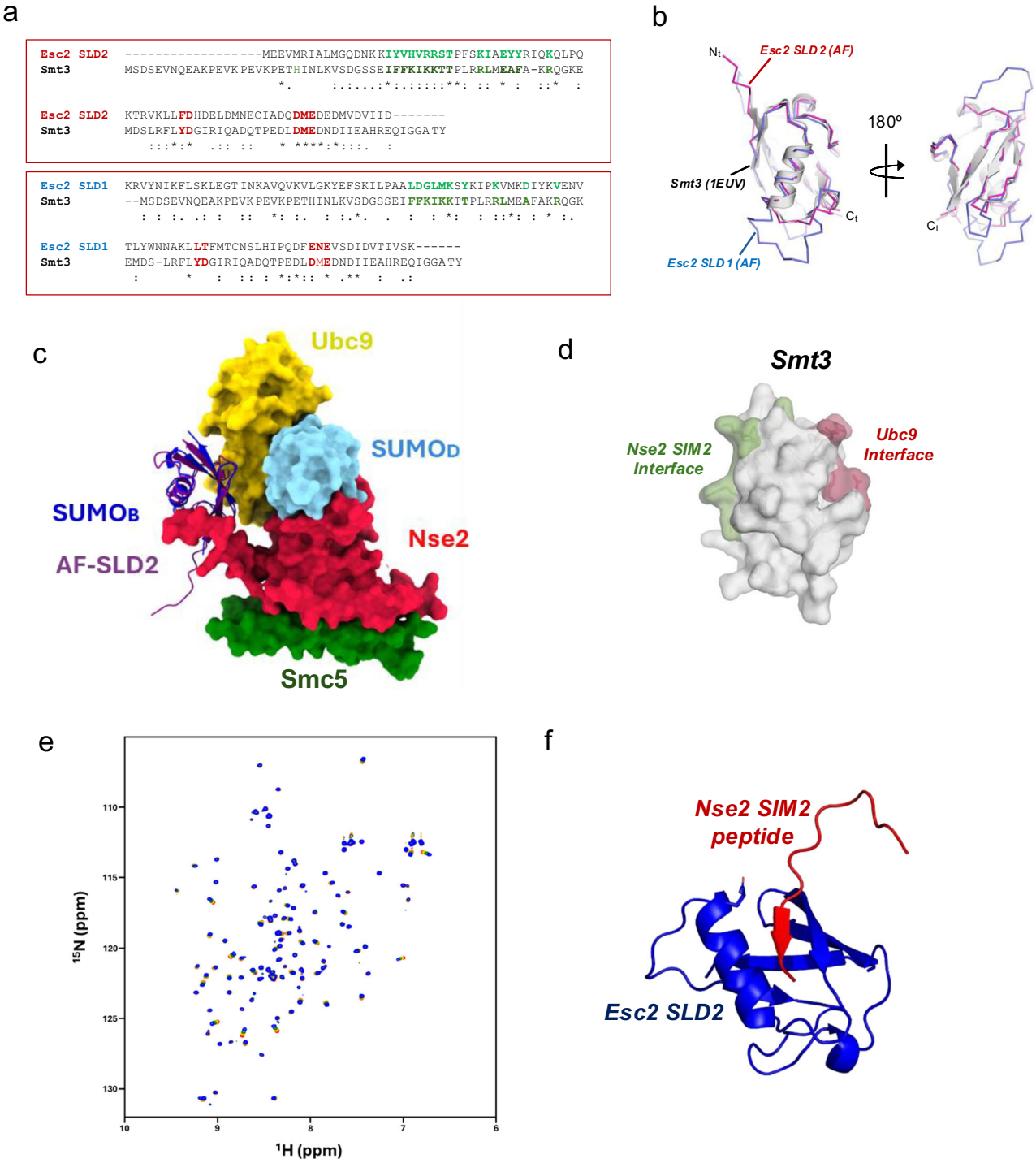

Fig. 1 | Structural and sequence comparisons of ESC2 and yeast SUMO (Smt3). **a** Sequence alignment of Esc2 SLD1 and SLD2 domains with Smt3 generated using Clustal Omega. Asterisks indicate fully conserved residues. SUMO residues involved in the Ubc9 and SIM2 interfaces are highlighted in red and green, respectively. **b** Structural superposition of AlphaFold-predicted Esc2 SLD1 (blue) and SLD2 (red) domains with Smt3, yeast SUMO (white, PDB code 1EUV). Two views related by a 180° rotation are shown. **c** Structural alignment of the SUMO backside ($SUMO_B$) with the AlphaFold SLD2 model of Esc2 positioned within the yeast Nse2/Arm-Smc5 complex bound to an E2-SUMO-donor ($SUMO_D$) thioester mimetic (PDB 7P47). **d** Surface representation of the Smt3 structure, highlighting the binding interfaces with Ubc9 and the SIM2 motif of Nse2, shown in red and green, respectively. **e** Superposition of the various $Esc2_{374-456}$ (SLD2 domain) 2D ^{1}H–^{15}N HSQC spectra from each titration point with the 13-mer SIM-containing peptide, showing the chemical shift perturbations for the different molar ratios (red 1:0; orange 1:0.5; yellow 1:1; green 1:2; blue 1:4). **f** AlphaFold model of the complex Esc2 SLD2:SIM-peptide of Nse2.

wild-type Smt3, used to engage the SUMO E2 backside interaction, with various Esc2 truncation constructs in the E3 ligase reaction mediated by Nse2/Arm-Smc5 (Fig. 3a). Notably, all three Esc2 constructs promoted E2 thioester discharge on the substrate to a degree comparable to that observed with the addition of extra Smt3. This suggests that the Esc2 SLD2 domain exerts a functional effect similar to Smt3 in facilitating E2 activity. We previously reported that E2~SUMO thioester discharge to the substrate is enhanced by the binding of a second SUMO molecule to the E2 backside during E3 ligase-catalyzed reactions involving Nse2/Arm-Smc5[13]. In our current in vitro assays, performed under less restrictive conditions using

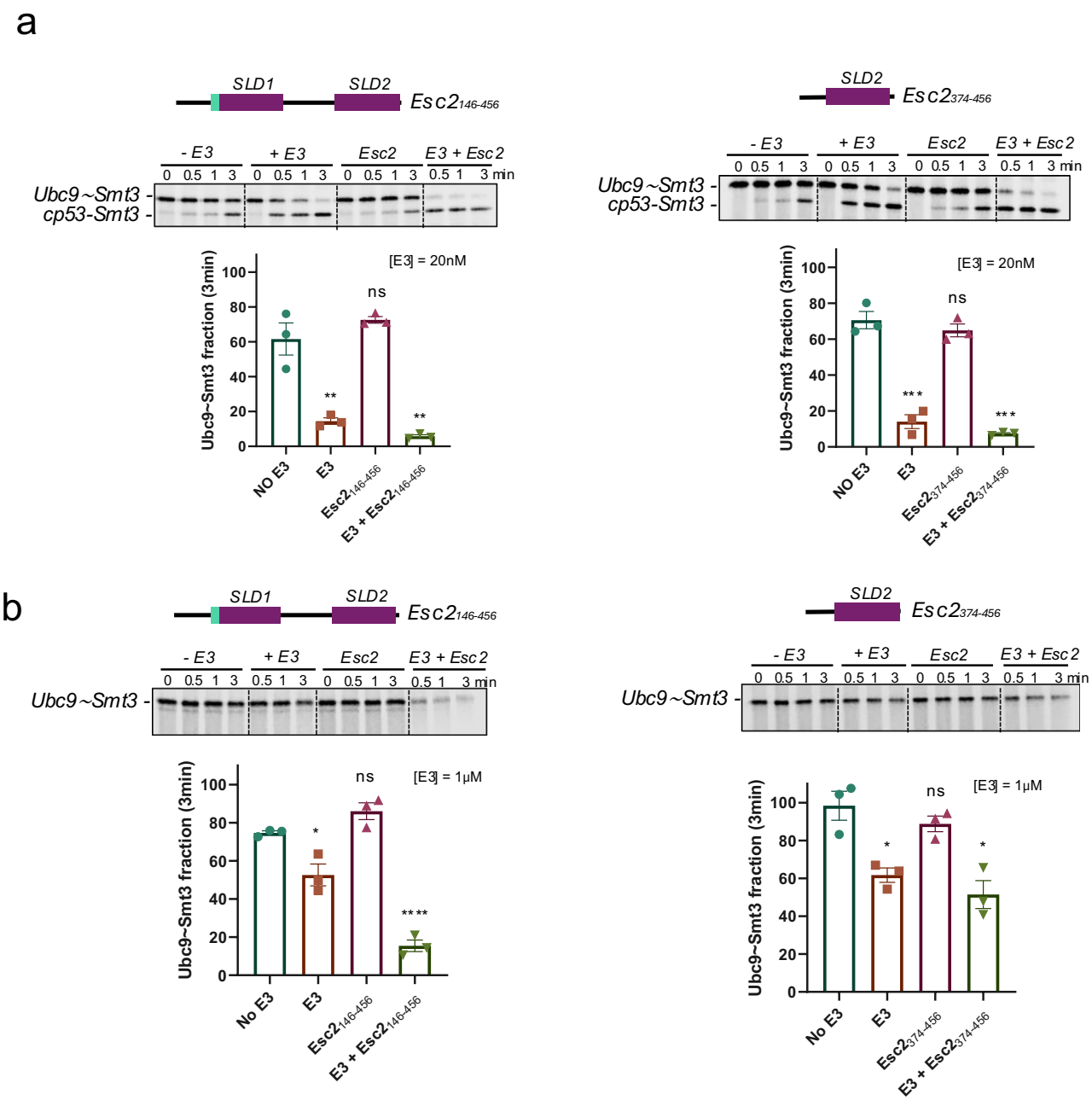

Fig. 2 | Esc2 does not function as a SUMO E3 ligase. Single-turnover SUMOylation reactions using *IRDye*-labeled D68R Smt3~Ubc9 thioester were performed in the absence or presence of Nse2/Arm-Smc5, Esc2 truncations, or both. Reactions were carried out with cp53 as substrate (**a**) or without substrate (**b**). Bar plots show the fraction of remaining D68R Smt3~Ubc9 thioester after 3 min. Data are presented as mean ± s.e.m. ($n = 3$ technical replicates). Statistical significance was assessed using a two-tailed unpaired *t* test, with the *No E3* sample used as the reference. All statistical analyses were performed at a 95% confidence interval. $^{*}P < 0.05$, $^{**}P < 0.01$, $^{***}P < 0.001$, $^{****}P < 0.0001$, ns: not significant. Exact *P* values from the left to right: **a** 0.0075, 0.3090, 0.0038; 0.0008, 0.3972, 0.0002; **b** 0.0191, 0.0663, <0.0001; 0.0128, 0.3342, 0.0116. Source data are provided in the Supplementary Data file.

5 nM Nse2/Arm-Smc5, we observed a similar enhancement of E2~SUMO thioester discharge mediated by all three Esc2 constructs, each exhibiting comparable activity (Fig. 3b). This supports the SLD2 domain as the key region within Esc2 responsible for promoting SUMO E3 ligase-dependent discharge, consistent with its structural resemblance to Smt3.

SLD2 of Esc2 binds Nse2 through the SIM2 motif

A detailed structural comparison between the AlphaFold3 model of the Esc2 SLD2 domain and Smt3 reveals substantial sequence conservation and structural similarity across two key interfaces: the SUMO-E2 interaction surface and the SIM-binding interface at the C-terminus of the E3 ligase Nse2 (Fig. 1). Notably, structural alignment of Esc2 SLD2 onto the Smt3^{B} position within the product complex structure of Nse2/Arm-Smc5 bound to the E2-SUMO thioester mimetic, together with biochemical evidence showing that SLD2 efficiently substitutes for Smt3 in conjugation assays (Figs. 1c and 4a), supports a model in which Esc2 SLD2 functions as a backside interactor that modulates E3 ligase activity of Nse2.

To evaluate the contribution of the SIM2 motif to SUMOylation, we conducted single-turnover assays using a C-terminal truncation mutant of the E3 ligase lacking the four terminal SIM2 residues, ΔSIM2Nse2/Arm-Smc5. This deletion is known to disrupt the SUMO-E2 backside interaction and impair E2~SUMO thioester discharge[13]. Consistent with this, our

results showed that the ΔSIM2Nse2 mutant displayed a markedly reduced ability to enhance SUMO transfer to the substrate, even in the presence of Esc2 SLD2 (Fig. 4b), demonstrating that Esc2-mediated stimulation depends on an intact SIM2 region. To corroborate this requirement, we examined a point mutation in Nse2/Arm-Smc5 (V266R), which likewise disrupts the Smt3 backside interaction[13]. V266R-Nse2 variant similarly failed to promote SUMO discharge in the presence of Esc2 SLD2 (Fig. 4c), reinforcing the necessity of SIM2 for Esc2-driven activation of the Nse2.

To refine our understanding of this interface, we analyzed single-point mutations in Esc2 SLD2 (H399E, R401D, and K408E), targeting residues that correspond to the conserved positively charged surface of SUMO involved in SIM recognition[13] (Fig. 4d). Single-turnover assays revealed a significant reduction in SUMO transfer efficiency for these mutants, underscoring the functional importance of this electrostatic surface (Fig. 4e). We next examined the contribution of these residues to peptide binding by performing NMR titrations with $Esc2_{374–456}$ triple mutant (H399E/R401D/K408E) (hereafter referred as *esc2-EDE*). In contrast to the wild-type protein, no significant CSPs were detected upon addition of the 13-mer SIM-containing peptide, even at the highest molar ratio tested (Fig. 4f). These results indicate that disruption of the conserved positively charged surface abolishes detectable binding to the Nse2 SIM2 motif and provide strong evidence for a direct association between Esc2 SLD2 and SIM2 that contributes to the stimulation of Nse2 E3 ligase activity. Taken together, the consistent loss of activity observed for both Nse2 and Esc2 SLD2 mutants demonstrates that perturbation of either binding surface compromises SUMO discharge, supporting a specific and functionally important SLD2-SIM2 interaction.

In addition, we recapitulated these single-turnover reactions using the composite hexameric form of the Smc5/6 complex, in which Nse2 is fully integrated with all the other subunits (Fig. 5a and Supplementary Fig. 4). In this context, the Esc2 SLD2 also enhanced E2~SUMO thioester discharge during the E3-dependent SUMOylation reaction. This stimulatory effect was compromised either by deletion of the C-terminal SIM2 motif of Nse2 (Fig. 5b) or by the introduction of a triple point mutation in Esc2 SLD2 (H399E, R401D, and K408E) (*esc2-EDE*) (Fig. 5c). In both cases, the SIM-mediated interface between Nse2 and Esc2 SLD2 is disrupted. Together, these findings support a unified model in which Esc2 SLD2 acts as a SUMO-like cofactor, at least for the Nse2 E3 ligase, stabilizing the E2-E3 complex and promoting substrate SUMOylation via a backside-binding mechanism.

The yeast Siz1 E3 ligase is not enhanced by Esc2

To determine whether the Esc2-mediated stimulation of SUMOylation is specific to Nse2 or might extend to other SUMO E3 ligases, we expanded our analysis to include yeast Siz1. Yeast Siz1 belongs to the same SUMO E3 ligase family and contains a SP-RING domain[36]. This allowed us to test whether Esc2 could enhance SUMO transfer in a distinct E3 context. In single-turnover assays under the same conditions, Esc2 failed to stimulate SUMOylation when Nse2 was replaced by Siz1 (residues 167–508, encompassing the C-terminal SIM that interacts with SUMO at the Ubc9 backside[12]). This was observed using both the p53 C-terminal region (previously shown to be a Siz1 substrate in vitro[36]) and also using the canonical Siz1 substrate PCNA (Supplementary Figs. 5 and 6).

These results indicate that the Esc2-dependent enhancement is not a general feature of SP-RING SUMO E3 ligases. Instead, these results highlight the specificity of the Esc2-Nse2 interaction, consistent with the idea that Esc2 functions as a dedicated E2 cofactor for Nse2. This selectivity likely reflects underlying structural and mechanistic distinctions among SUMO E3 ligases.

The Esc2-Nse2 SIM2 interaction acts synergistically with Mms4 and Slx4 to maintain genome integrity

Our next step was to check the relevance of the Esc2-Nse2 SIM2 interface in vivo. We thus conducted yeast viability assays comparing wild-type ESC2 with the esc2-EDE triple mutant, which disrupts the SIM2 interaction, and challenged cells with different DNA-damaging agents: methyl methanesulfonate (MMS), 4-NQO (4-nitroquinoline N-oxide), or UV radiation. Previous work has shown that disruption of the Esc2 SLD2 interface with Ubc9 causes little or no phenotype on its own, but becomes critical in the absence of other DNA repair factors, such as the nucleases Mms4 or Slx4, which resolve recombination intermediates, including Holliday junctions (HJs) and stalled replication forks, generated during DNA repair[24,26]. Similarly, truncation of the Nse2 C-terminal SIM2 produces a similar synthetic sensitivity with *mms4* or *slx4* mutants[13]. Esc2 has been reported to be involved in the dissolution of HJs at damaged replication forks by enhancing the Nse2-Smc5-dependent SUMOylation of members of the STR complex (Sgs1-Top3-Rmi1)[27–29]. Thus, although the functional link between Esc2 and Nse2-Smc5 to enhance SUMO conjugation of DNA repair factors has been established, a direct interaction between Esc2 and the Smc5/6 complex remains uncertain.

To further explore the functional connection between the C-terminal SIM2 of Nse2 and the Esc2 SLD2 domain, we assessed the DNA-damage sensitivity of the *esc2-EDE* mutant in combination with deletions of *MMS4* or *SLX4* (Fig. 6a). Serial dilution assays showed that *esc2-EDE* cells displayed no obvious growth defect and no intrinsic sensitivity to DNA-damaging agents. However, when combined with *mms4Δ* or *slx4Δ*, the *esc2-EDE* mutation caused a synergistic increase in MMS sensitivity, phenocopying the synthetic effects observed when the Esc2-Ubc9 interface is disrupted. This interaction must also be important when replication forks stall at natural protein-DNA barriers, as the *esc2-EDE* mutant also increased the DNA damage sensitivity of *rrm3Δ* cells. These findings reinforce the role of Esc2 in DNA repair pathways by enhancing the SUMO E3 ligase activity of Nse2, which depends on interactions with both Ubc9 and the SIM2 motif.

Finally, and in contrast to the synthetic interaction observed with *mms4Δ*, *slx4Δ* or *rrm3Δ*, the *esc2-EDE* mutant did not exacerbate the DNA-damage sensitivity of an *sgs1Δ* mutant strain (Fig. 6b). To directly assess whether the Esc2-SIM2 interaction promotes the STR complex SUMOylation in vivo, we performed SUMO pull-down assays in cells expressing 6His-Smt3 and 9Myc-tagged Sgs1 or 6HA-tagged Top3 following MMS treatment. Under these conditions, SUMO-conjugated Sgs1 and Top3 were readily detected in wild-type cells but were markedly reduced in the *esc2-EDE* mutant, indicating that the Esc2-SIM2 interaction contributes to efficient Sgs1 and Top3 SUMOylation in response to replication fork damage (Fig. 6c, d). These observations are consistent with the Esc2-Nse2 SIM2 interaction functioning upstream of Sgs1 to promote SUMOylation and STR-mediated dissolution of recombination intermediates. In contrast, loss of the backup Mms4-Mus81/Slx4 nuclease pathways renders cells dependent on Esc2-Nse2 function under genotoxic stress, indicating that the SIM2-mediated interaction acts redundantly with nuclease-mediated resolution to maintain genome integrity.

Discussion

SUMOylation affects hundreds of protein substrates in the cell, thereby regulating multiple pathways, particularly within the nucleus. In contrast to the large number of ubiquitin E3 ligases, the SUMOylation pathway comprises only a few well-characterized SUMO E3 ligases, which primarily enhance the SUMO transfer reaction rather than provide extensive substrate specificity. In the yeast nucleus, Siz1, Siz2, and Nse2 are the only well-established SUMO E3 ligases known to regulate the activity of numerous protein substrates. They enhance the E2~SUMO discharge reaction by means of the conserved SP-RING domain and adjacent SIM motifs, which restrain the conformation flexibility of the E2~SUMO thioester conjugating enzyme, thereby facilitating the formation of the isopeptide bond with the substrate. In yeast, a "spray" or "group" SUMOylation mechanism has been proposed, which restricts SUMO conjugation to specific cellular compartments through the formation of a highly active E3–E2~SUMO thioester complex[37]. An alternative mechanism for regulating E2~SUMO discharge may involve interactions with cofactors such as budding yeast Esc2, *S. pombe* Rad60, and human Nip45. These cofactors typically bind to the backside of the SUMO E2-conjugating enzyme, and they may act in concert with SUMO E3 ligases by modulating their activity through allosteric effects.

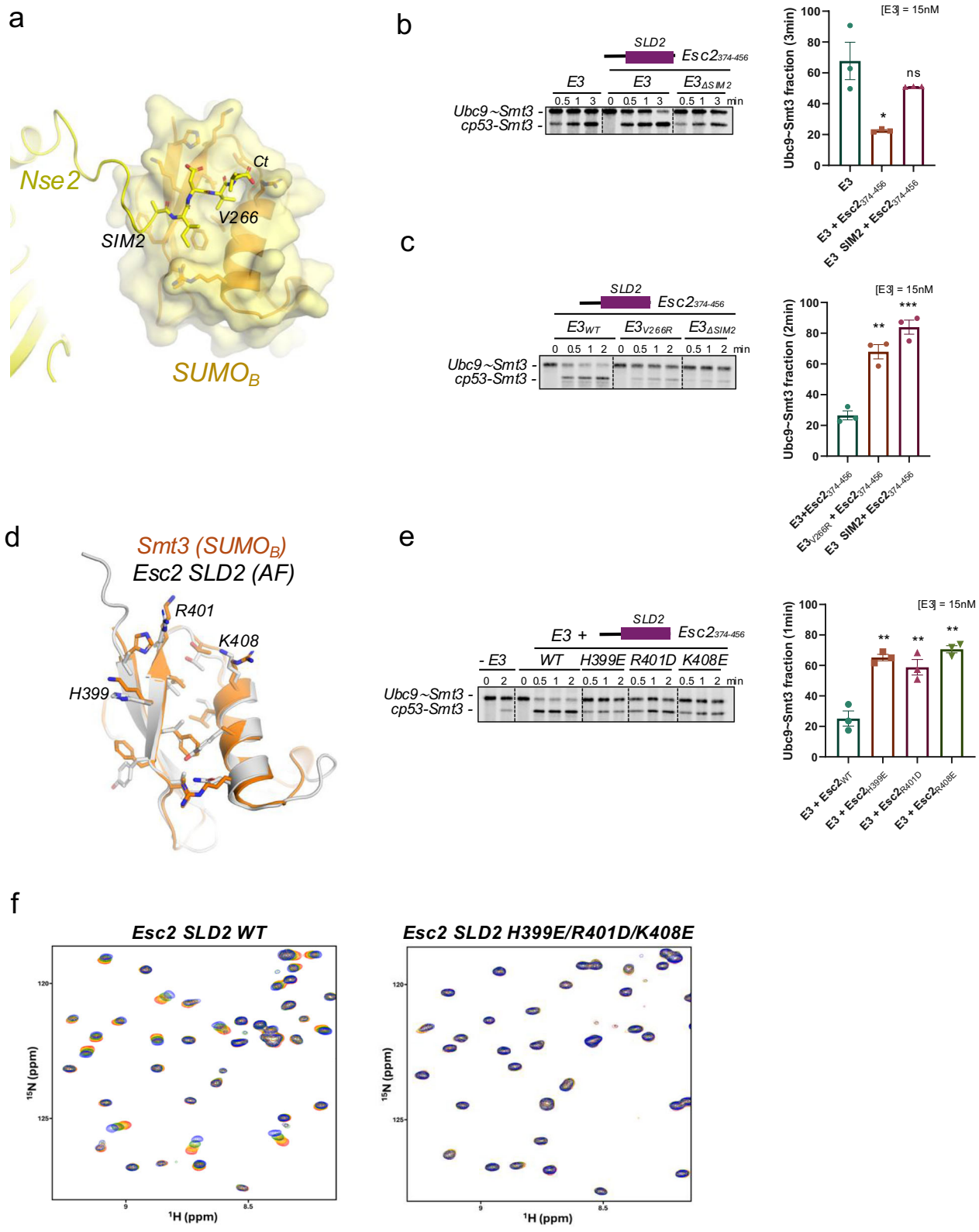

Yeast Esc2 facilitates SUMO conjugation on substrates involved in resolving stalled or entangled DNA structures, such as Holliday junctions (HJ) and replication forks, thereby contributing to genome stability[38]. Esc2 typically acts in concert with the Smc5/6 complex by enhancing the SUMO E3 ligase activity of its Mms21 (Nse2) subunit and promoting SUMOylation of DNA repair factors, including Pol2 and the STR complex (Sgs1-Top3-Rmi1), which is essential for HJ dissolution. Notably, Esc2 preferentially binds to entangled DNA regions, such as HJs, rather than standard dsDNA[20,39], supporting its proposed role as a DNA-specific regulator of SUMO conjugation[38]. Multiple studies further demonstrate that Esc2 selectively enhances the Mms21/Nse2 branch of the SUMO pathway, with *esc2Δ* or *Esc2-SLD2* mutants mirroring *nse2* mutant defects while having minimal impact on Siz1/Siz2-dependent SUMOylation. Together, these findings establish Esc2 as a dedicated Ubc9-binding cofactor that

Fig. 4 | Esc2 binds the C-terminal SIM2 of the Nse2 E3 ligase and enhances SUMO conjugation. a Structure of the SUMO backside in complex with the C-terminal SIM2 motif of Nse2, derived from the Nse2/Smc5–E2~SUMO thioester complex (PDB 7P47). SIM2 is shown in yellow. **b** Left: Single-turnover in vitro SUMOylation assays monitoring thioester discharge in the presence of cp53 using wild-type or ΔSIM2 Nse2/Arm-Smc5, with $Esc2_{374-456}$. **c** As in (**b**), comparing wild-type, V266R, and ΔSIM2 Nse2/Arm-Smc5 variants. **d** Structural alignment of AlphaFold-predicted Esc2 SLD2 with Smt3 (PDB 1EUV). Residues contacting SIM2 are shown in sticks. **e** As in (**b**), using $Esc2_{374-456}$ wild-type or point mutants (H399E, R401D, or R408E). Bar plots show the fraction of remaining *IRDye*-labeled D68R Smt3~Ubc9 thioester at the indicated time points. Data are presented as mean ± s.e.m. ($n = 3$ technical replicates). Statistical significance was assessed using a two-tailed unpaired *t* test, with the *E3*, *E3+Esc2374-456*, or *E3+Esc2WT* sample used as the reference. All statistical analyses were performed at a 95% confidence interval. $^{*}P < 0.05$, $^{**}P < 0.01$, $^{***}P < 0.001$, $^{****}P < 0.0001$, ns: not significant. Exact *P* values from the left to right: **b** 0.0204, 0.2401; **c** 0.0017, 0.0004; **e** 0.0018, 0.0091, 0.0012. Source data are provided in the Supplementary Data file. **f** Superposition of the various $Esc2_{374-456}$ WT (left, zoomed up spectra of Fig. 1e, reproduced for comparison at the same scale) and $Esc2_{374-456}$ triple mutant (H399E, R401D, and R408E) (right) 2D ^{1}H–^{15}N HSQC spectra from each titration point showing the chemical shift perturbations for the different molar ratios (red 1:0; orange 1:0.5; yellow 1:1; green 1:2; blue 1:4).

specifically boosts Nse2 activity, rather than functioning as a broad stimulator of Siz/PIAS-type SUMO E3 ligases[24,26,40].

Our findings are consistent with those of previous studies and support the conclusion that the SLD2 domain of yeast Esc2 enhances the SUMO E3 ligase activity of Nse2/Mms21 by acting as a cofactor for the E2 conjugating enzyme. Since Esc2, and its orthologs Rad60 and Nip45, directly interact with the SUMO E2 through their SUMO-like domains and promote E2~SUMO thioester discharge onto substrates, they have also been proposed to be E3 ligases[23]. However, in our in vitro assays, the presence of Esc2 alone does not appreciably stimulate SUMO transfer or significantly reduce the E2~SUMO thioester levels, although we cannot rule out the possibility that Esc2 may act as an independent E3 ligase under specific conditions or with particular substrates. What we do observe is a marked enhancement of Nse2's SUMO E3 ligase activity in the presence of the Esc2's SLD2 domain, an enhancement that strongly suggests a cofactor role and is comparable to the stimulation provided by SUMO binding to the E2 backside during catalysis.

The structure of the Nse2/Arm-Smc5 E3 ligase bound to an E2~SUMO thioester mimetic revealed two SUMO-interacting motifs (SIMs) in Nse2 that are essential for catalysis: SIM1, which engages the SUMO donor, and SIM2, located at the C-terminus, which interacts with the E2 SUMO backside[13]. SIM1 is critical for SUMO conjugation and indispensable for yeast viability under DNA damage stress. In contrast, the absence of SIM2 significantly reduces E3 activity and is only required for viability when combined with other DNA damage factors, such as *mms4* or *slx4*[13]. Notably, combining an Esc2 SLD2 point mutant (unable to bind the Ubc9 backside) with *MMS4* or *SLX4* deletions causes similar severe viability defects under DNA damage conditions[24,26]. These findings support the model that Esc2's SLD2 domain binds the Ubc9 backside to promote E2~SUMO thioester discharge on specific targets during DNA repair, similar to the stimulatory effect conducted by the non-covalent SUMO binding to the Ubc9 backside.

Our findings reveal a possible molecular mechanism by which Esc2 enhances the SUMO E3 ligase activity of Nse2. This occurs via its interaction with the E2 backside during the E3-catalyzed product complex, stabilizing an optimal thioester conformation that promotes efficient discharge onto DNA repair protein factors. Interestingly, since human Nse2 lacks the C-terminal SIM motif, an alternative mode of interaction has been proposed for Nip45[41]. In vitro single-turnover conjugation assays show that defects in E2~SUMO discharge at the SLD2–SIM2 binding interface closely resemble those observed in the SIM2 deletion mutant and in the SIM2 V266R variant. Consistently, yeast complementation assays demonstrate similar viability defects caused by mutations in the SLD2 surfaces interacting with Ubc9, with the Nse2 SIM2, and by a SIM2 deletion mutant in Nse2.

We propose a model in which the Smc5/6 complex is recruited to DNA repair sites, including Holliday junction and stalled/damaged forks, to SUMOylate specific DNA repair factors, such as the STR complex (Fig. 7). This activity would be required to promote the STR-dependent resolution pathway during S phase and, in its absence, would require the processing of junctions by the Mms4-Mus81 and Slx4 nucleases in mitosis. Our results indicate that this SUMOylation activity is modulated by Esc2, which is also recruited to recombination intermediates and interacts with the E2 enzyme's backside in the E2-E3 complex to enhance the SUMO conjugation activity of Nse2 in an allosteric manner. By promoting Smc5/6-dependent SUMOylation at sites of DNA damage, Esc2 adds a layer of control on sister chromatid disjunction activities, contributing to the maintenance of genome stability.

Methods

Plasmid construction for overexpression in bacterial cells

Cloning of mature yeast SUMO (SMT3), the SMT3 K11C/D68R mutant, yeast E1 (AOS1/UBA2ΔC-term, residues 1–554), yeast E2 (UBC9 and the K153R mutant), yeast E3 full-length NSE2 and mutants, and the SMC5 Arm construct (residues Asp302–Thr366 and Arg737–Gln813) has been described previously[12,13,36,42]. Yeast E3 active fragment SIZ1 (residues 167–508) was cloned into pET28a using the NdeI and XhoI restriction sites. Full-length *S. cerevisiae* Esc2 (S288c) cloned into pET28a was used as a template for site-directed mutagenesis to generate three C-terminal truncation constructs ($Esc2_{146-456}$, $Esc2_{191-456}$, and/or $Esc2_{374-456}$) by deletion of the N-terminal coding region. Yeast PCNA cDNA was cloned into a pET151D-TOPO vector. Full-length SMC5 and SMC6 were cloned into the pET28a and pET15 expression vectors, respectively. NSE1–NSE4 were encoded on a pCDFDuet vector containing two T7 promoters and ribosome-binding sites.

Protein expression and purification

Recombinant proteins were expressed in *E. coli* Rosetta2 (DE3) cells (Novagen). For Nse2/Arm-Smc5 complexes, 6×His-tagged Nse2 variants were co-expressed with untagged Arm-Smc5. Cultures were grown at 37 °C to an OD_{600} of ~0.6, induced with 0.5 mM IPTG, and incubated for 16 h at 20 °C. Cells were harvested, resuspended in lysis buffer (50 mM Tris-HCl pH 8.0, 350 mM NaCl, 20% sucrose, 20 mM imidazole, 1 mM β-mercaptoethanol, 0.1% IGEPAL), lysed by sonication, and clarified by centrifugation (21,000×*g*, 15 min). The full-length hexameric complex was generated by co-expression of three plasmids under similar conditions.

His-tagged proteins and complexes were purified by immobilized metal affinity chromatography using Chelating Sepharose Fast Flow resin (Cytiva) and eluted with 250 mM imidazole. Nse2/Arm-Smc5 and the hexameric complexes were further purified by size-exclusion chromatography on a Superdex 200 HiLoad column (Cytiva).

Esc2 constructs ($Esc2_{146-456}$, $Esc2_{191-456}$, and $Esc2_{374-456}$), the cp53 substrate (Lys320–Asp393), yeast E1 (Aos1:Uba2ΔC-term, residues 1–554), yeast E2 (Ubc9, wild-type and K153R), and yeast SUMO (Smt3, wild-type and K11C/D68R mutant) were individually expressed and purified following the same general protocol.

Siz1 was purified by metal affinity chromatography followed by dialysis to reduce salt concentration and anion-exchange chromatography on a Resource Q column (Cytiva) equilibrated in 20 mM HEPES pH 8.0, 30 mM NaCl, and 1 mM β-mercaptoethanol, with elution using a 30–500 mM NaCl gradient.

PCNA was purified by metal affinity chromatography and further purified by size-exclusion chromatography on a Superdex 75 HiLoad

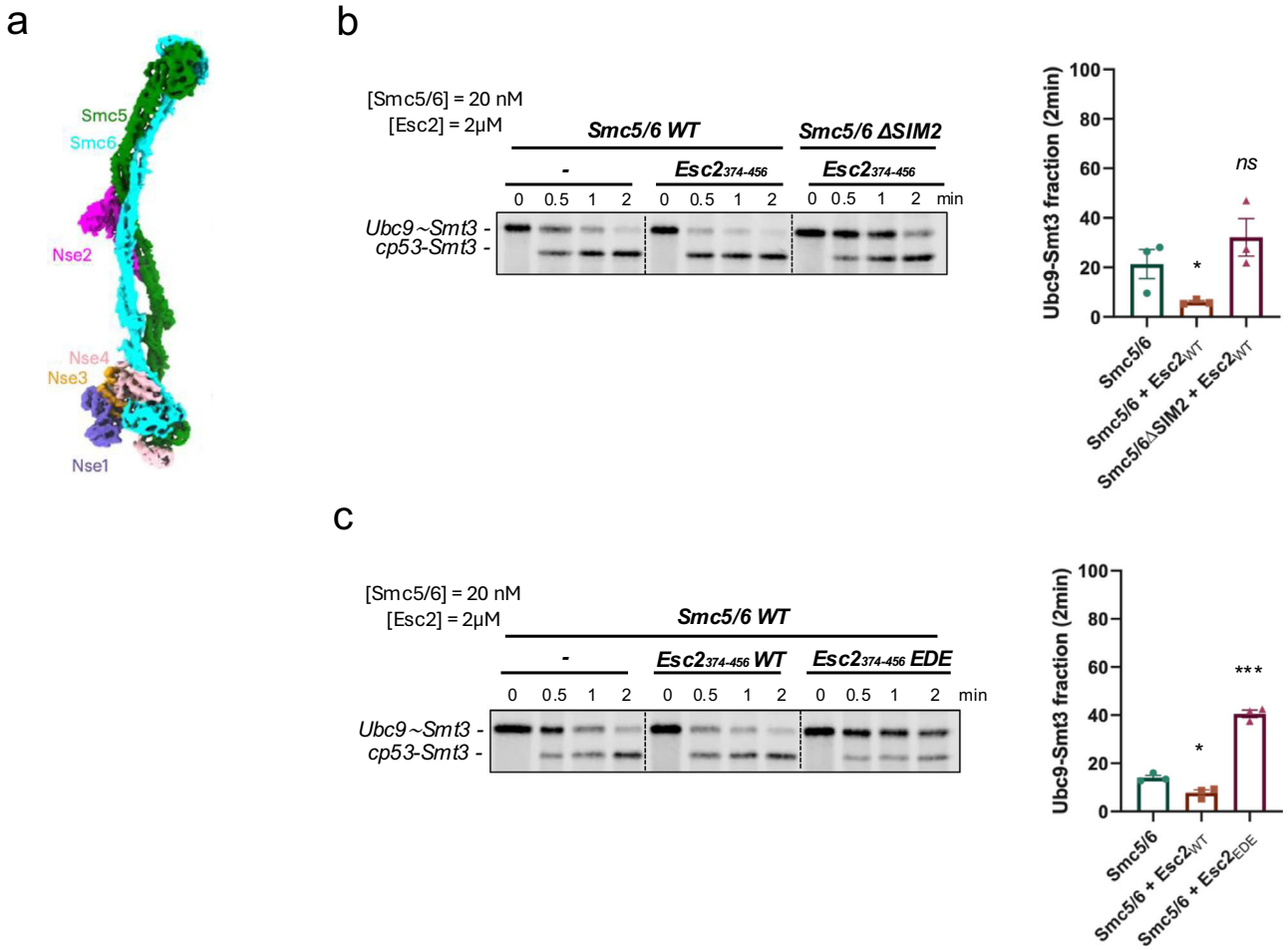

Fig. 5 | Esc2 enhances SUMO E3 ligase activity of Nse2 in the context of the hexamer Smc5/6 complex. a CryoEM structure of the yeast hexamer Scm5/6 complex (PDB code 8I13). **b** Single-turnover in vitro SUMOylation assay monitoring thioester discharge in the presence of cp53 using wild-type or ΔSIM2 Nse2 in the context of the hexamer Smc5/6 complex, with $Esc2_{374-456}$. **c** As in (**b**), comparing $Esc2_{374-456}$ wild-type and triple mutant (H399E, R401D, and R408E). Bar plots show the fraction of remaining *IRDye*-labeled D68R Smt3~Ubc9 thioester at the indicated time points. Data are presented as mean ± s.e.m. ($n = 3$ technical replicates). Statistical significance was assessed using a two-tailed unpaired *t* test, with the *Smc5/6* sample used as the reference. All statistical analyses were performed at a 95% confidence interval. $^{*}P < 0.05$, $^{**}P < 0.01$, $^{***}P < 0.001$, $^{****}P < 0.0001$, ns: not significant. Exact *P* values from left to right: **a** 0.0307, 0.2137; **b** 0.0049, 0.0098. Source data are provided in the Supplementary Data file.

column (Cytiva) equilibrated in 250 mM NaCl, 20 mM Tris pH 8.0, and 1 mM β-mercaptoethanol.

Smt3 labeling with IRDye 800CW

Mature Smt3 (K11C/D68R) were fluorescent labeled using IRDye 800CW Maleimide according to the manufacturer's instructions (LI-COR). Protein was diluted in 20 mM HEPES pH 7.2, 50 mM NaCl, 0.5 mM TCEP up to 40 μM. IRDye 800CW Maleimide stock solution was added gently to reach a 20:1 ratio. Mixtures were kept at 4 °C for 16 h. Free probe molecules were removed using a PD-10 desalting column (Cytiva), followed by ten times the volume washing by Centricon (MerckMillipore) centrifugation equilibrated on the same HEPES buffer. Proteins were concentrated up to 1–2 mg/mL and flash frozen prior to use.

Expression and purification of ^{15}N isotopically labeled $yEsc2_{374-456}$ WT and $yEsc2_{383-456}$ triple mutant (H399E, R401D, and R408E)

The plasmids containing the sequence for $Esc2_{374-456}$ WT or $Esc2_{383-456}$ triple mutant (H399E, R401D, and R408E) were transformed into *E. coli* strain BL21 (DE3) using kanamycin selection (50 mg/L), and the ^{15}N-labeled protein was expressed in defined isotopically labeled M9 minimal media with $^{15}NH_4Cl$ as the sole nitrogen source (Reed et al., 2003). The cells were grown at 37 °C with shaking until $OD_{600nm} = 0.8$, at which point they were cooled to 20 °C and induced with IPTG to a final concentration of 0.5 mM. The cultures were incubated with shaking for a further 16 h and were harvested by centrifugation. The cell pellet was resuspended, and protein purification was performed as previously described.

NMR spectroscopy

A 5-mm NMR tube was loaded with 100 mM ^{15}N-labeled $yEsc2_{374-456}$ WT or $yEsc2_{383-456}$ triple mutant (H399E, R401D, and R408E) in NMR buffer (50 mM KPi, pH 7.0, 50 mM NaCl, 5 mM DTT, 0.1 mM EDTA, 2 mM NaN_3, 10% D_2O) supplemented with 1 mM trimethylsilyl propanoic acid (TSP) as a chemical shift reference (0 ppm). The 2D ^{1}H–^{15}N HSQC experiments were recorded at 298 K using a 600 MHz Bruker Neo 4-channel spectrometer fitted with a 5-mm TCI cryoprobe equipped with z-axis gradients and running TopSpin software version 4.0.5.

Single-turnover conjugation assays

Reactions were performed essentially as described previously[13], with minor modifications. The E2~SUMO thioester was generated in a reaction mixture containing 40 mM HEPES pH 7.5, 25 mM NaCl, 10 mM $MgCl_2$, 0.1% Tween-20, 0.1 mM DTT, 0.2 μM yeast E1, 2 μM yeast E2 (Ubc9 K153R), and 2 μM IRDye-labeled Smt3 K11C/D68R. Reactions were initiated by the

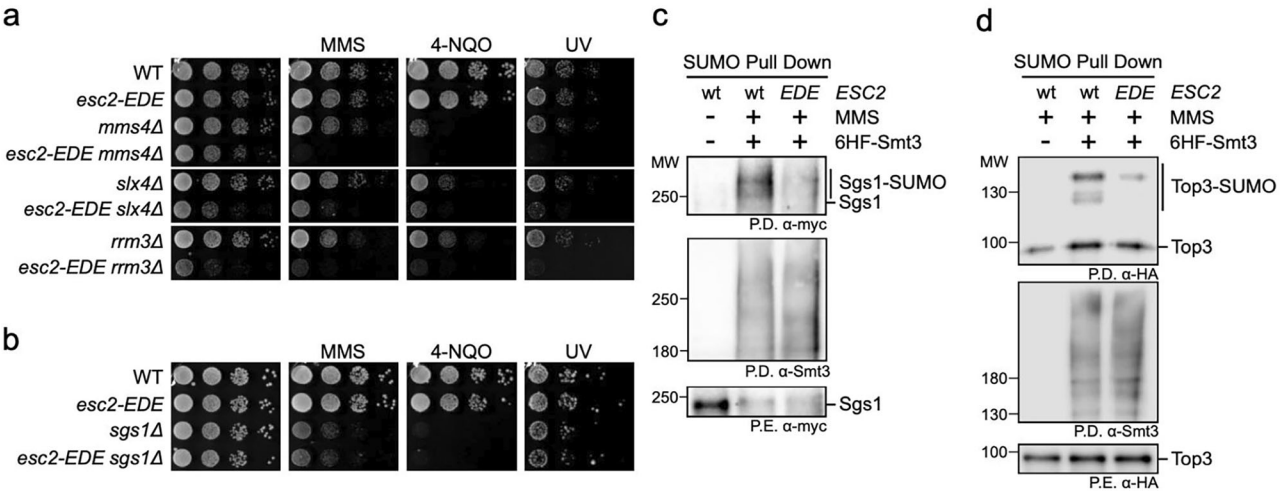

Fig. 6 | The Esc2-Nse2 SIM2 interaction acts synergistically with Mms4, Slx4 and Rrm3 to maintain genome integrity. a Growth test analysis of *esc2-EDE* cells in combination with *mms4Δ*, *slx4Δ* and *rrm3Δ*; tenfold serial dilutions of liquid cultures were spotted in YPD in the presence of either MMS (0.0025%), 4-NQO (50 ng/ml), or irradiated with UV (40 μJ/m^2) and incubated at 30 °C for 48 h. **b** Growth test analysis of *esc2-EDE* cells in combination with *sgs1Δ*. Same doses for genotoxic agents as in (**a**). **c** Exponentially growing wild-type (wt) or *esc2-EDE* cells expressing C-terminally 9Myc-tagged Sgs1 and either expressing (+) or not (−) 6His-tagged Smt3 from their endogenous loci were analyzed. Where indicated (+), cultures were treated with 0.033% MMS for 2 h prior to harvesting. SUMOylated species were isolated from protein extracts (P.E.) by Ni-NTA pull-down (P.D.) under denaturing conditions. Sgs1-9Myc and SUMO-conjugated forms were detected by western blot. **d** Similar SUMO pull-down experiments as **c** comparing wild-type (wt) or *esc2-EDE* cells expressing C-terminally 6HA-tagged Top3. Source data are provided in the Supplementary Data file.

addition of 0.5 mM ATP, incubated at 30 °C for up to 5 min, and quenched by the addition of 2.5 mM EDTA.

For E3- or Esc2-mediated thioester transfer assays (Fig. 2), 15 μL of the preformed K153RUbc9~Smt3K11C/D68R-IRDye thioester was diluted twofold and supplemented with 0.8 μM 60-nt ssDNA, 8 μM cp53 (or PCNA), and either 20 nM Nse2/Arm-Smc5 or 20 nM Esc2 truncations ($Esc2_{146-456}$ or $Esc2_{374-456}$), alone or in combination. For thioester discharge assays in the presence of non-conjugatable Smt3 or Esc2 fragments (Figs. 3–5), reactions additionally contained 2 μM unlabeled Smt3 (WT) or all three Esc2 truncations (including $Esc2_{191-456}$), and 5–1000 nM Nse2/Arm-Smc5 or Siz1, as indicated.

All reactions were incubated at 30 °C, quenched at the indicated time points with non-reducing Laemmli buffer (Bio-Rad), resolved by non-reducing SDS–PAGE, and visualized by IRDye800CW fluorescence using a LI-COR Odyssey imaging system (v3.0).

Statistics and reproducibility

Band densitometry was performed using Empiria Studio® software. Data are presented as the mean ± s.e.m. of three technical replicates ($n = 3$). Statistical significance relative to the indicated sample was assessed using a two-tailed unpaired *t* test with a 95% confidence interval. $^*P < 0.05$, $^{**}P < 0.01$, $^{***}P < 0.001$, $^{****}P < 0.0001$, ns: not significant.

Construction of yeast mutant strains

All yeast strains were generated in the BY4741 genetic background. The *esc2-EDE* allele was constructed by PCR amplification of the C-terminal region of *ESC2* from a bacterial-expression plasmid, followed by fusion to a selectable marker and integration into the endogenous locus by HR. Correct integration was verified by PCR and DNA sequencing. Double-mutant strains carrying *esc2-EDE* in combination with *sgs1Δ*, *slx4Δ*, and *rrm3Δ* mutations were obtained by standard genetic crosses and sporulation.

Yeast growth test analysis

Ten-fold serial dilutions of exponentially growing yeast cultures were spotted onto solid media. Plates were incubated at the appropriate temperature for 2–3 days and imaged using a ChemiDoc Chemiluminescent Imager (Bio-Rad). MMS and 4-nitroquinoline 1-oxide (4-NQO) were added to YPD agar before solidification at final concentrations of 0.0025% and 50 ng/mL, respectively. For UV-induced damage, freshly spotted YPD plates were irradiated at a dose of 40 μJ/cm^2 and immediately wrapped in aluminum foil to prevent photoreactivation. Plates were then incubated at 30 °C until colonies were visible on the untreated control plates.

SUMO pull down from yeast extracts

SUMO pull-downs were performed under denaturing conditions from yeast strains expressing 6HisFlag-tagged Smt3 integrated at the endogenous *SMT3* locus. Exponentially growing cultures were treated with 0.033% MMS for 2 h prior to harvesting. For each pull-down, 100 OD_{600} units of cells were collected by centrifugation (3000 rpm, 2 min), washed once with cold water, and transferred to 1.5-ml tubes. Cell pellets were resuspended in 250 μl Buffer A (6 M guanidine hydrochloride, 100 mM KH_2PO_4, 10 mM Tris-HCl, 0.05% Tween-20, 15 mM imidazole, 1× protease inhibitors; pH 8.0) and mixed with 500 μl glass beads. Cells were disrupted using a mini-beadbeater (BioSpec Products; power 6, 1.5 min). Lysates were recovered by puncturing the bottom of the tube with a 21 G needle and centrifuging (2400 rpm) into a fresh tube. Beads were rinsed with 700 μl Buffer A, combined with the extract, and clarified by centrifugation (14,000 rpm, 10 min, 4 °C). The supernatant volume was adjusted to 1 ml with Buffer A. In total, 70 μl Ni-NTA agarose beads (Qiagen) were added to each sample and incubated overnight at room temperature on a rotating wheel. Beads were collected by centrifugation (3400 rpm) and washed three times (8 min each) with Buffer B (8 M urea, 100 mM KH_2PO_4, 10 mM Tris-HCl, 0.05% Tween-20, 2 mM imidazole; pH 8.0), followed by three washes with Buffer C (8 M urea, 100 mM KH_2PO_4, 10 mM Tris-HCl, 0.05% Tween-20; pH 6.3). Proteins bound to the beads were eluted by boiling for 3 min at 95 °C in 25 μl 2× sample buffer (4% SDS, 250 mM Tris-HCl pH 6.8, 10% sucrose, 0.02% bromophenol blue). For input controls, 30 μl of supernatant were precipitated with 12% TCA, washed three times with cold acetone, air-dried, resuspended in 30 μl Buffer B, incubated at 37 °C for 20 min, and mixed with 30 μl 2× sample buffer prior to boiling. Samples were resolved by SDS–PAGE and analyzed by western blot.

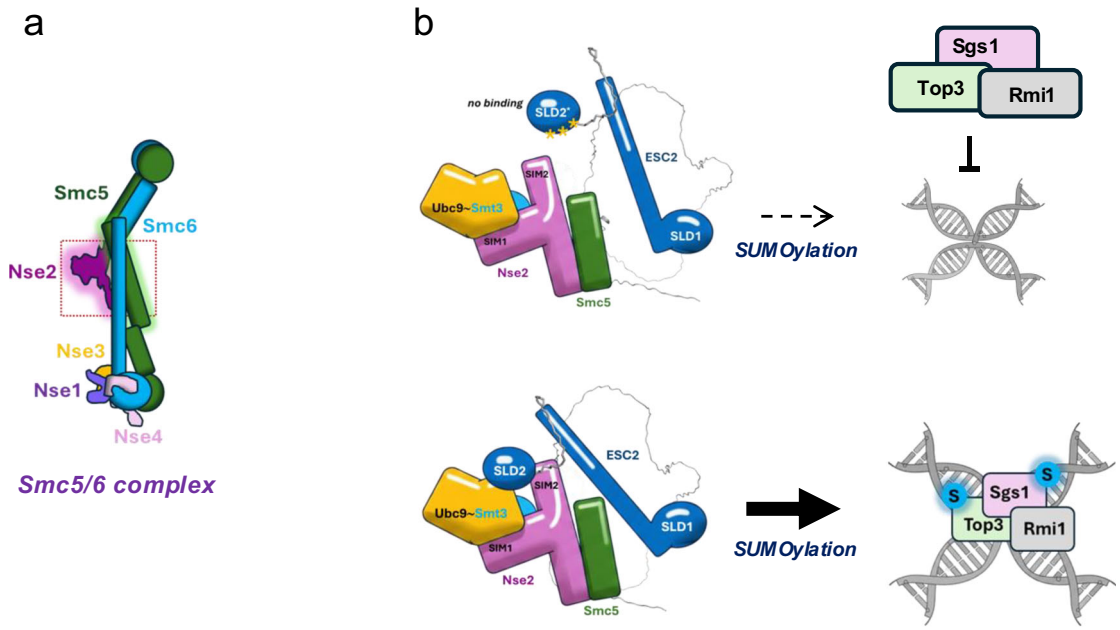

Fig. 7 | Model for binding of the Esc2 SLD2 domain within the Nse2/Arm-Smc5–E2~SUMO thioester complex. a Schematic representation of the hexameric Smc5/6 complex in a rod-shaped conformation, based on PDB 8I13. **b** Model of the Nse2/Arm-Smc5–E2~SUMO thioester complex with Esc2 SLD2 positioned at the Ubc9~SUMO backside. Proteins are labeled, and asterisks indicate Esc2 SLD2 residues mutated in this study that affect SIM2-dependent binding and SUMOylation enhancement (see Figs. 3 and 4).

Reporting summary

Further information on research design is available in the Nature Portfolio Reporting Summary linked to this article.

Data availability

Protein Data Bank accession code used in this study: 7P47 (Nse2/Smc5–E2~SUMO complex). Data sharing not applicable to this article as no datasets were generated or analyzed during the current study. All other data supporting the findings of this study are available within the article and its supplementary information files. Source data for Figs. 2, 3, 4, 5, and 6 and Supplementary Figs. 4, 5, and 6 are in the Supplementary Data file. Uncropped gel images for Figs. 2, 3, 4, 5, and 6 are available as Supplementary Figs. 7, 8, 9, 10 and 11.

Received: 16 February 2026; Accepted: 10 August 2026;
Published online: 24 August 2026

References

1. Bhachoo, J. S. & Garvin, A. J. SUMO and the DNA damage response. *Biochem. Soc. Trans.* **52**, 773–792 (2024).
2. García-Rodríguez, N., Wong, R. P. & Ulrich, H. D. Functions of ubiquitin and SUMO in DNA replication and replication stress. *Front. Genet.* **7**, 87 (2016).
3. Vertegaal, A. C. O. Signalling mechanisms and cellular functions of SUMO. *Nat. Rev. Mol. Cell Biol.* **23**, 715–731 (2022).
4. Wu, W. & Huang, C. SUMOylation and DeSUMOylation: prospective therapeutic targets in cancer. *Life Sci.* **332**, 122085 (2023).
5. Pichler, A., Fatouros, C., Lee, H. & Eisenhardt, N. SUMO conjugation —a mechanistic view. *Biomol. Concepts* **8**, 13–36 (2017).
6. Varejão, N., Lascorz, J., Li, Y. & Reverter, D. Molecular mechanisms in SUMO conjugation. *Biochem. Soc. Trans.* **48**, 123–135 (2019).
7. Lascorz, J., Codina-Fabra, J., Reverter, D. & Torres-Rosell, J. SUMO-SIM interactions: from structure to biological functions. *Semin. Cell Dev. Biol.* **132**, 193–202 (2022).
8. Song, J., Zhang, Z., Hu, W. & Chen, Y. Small ubiquitin-like modifier (SUMO) recognition of a SUMO binding motif: a reversal of the bound orientation*. *J. Biol. Chem.* **280**, 40122–40129 (2005).
9. Yau, T.-Y., Sander, W., Eidson, C. & Courey, A. J. SUMO interacting motifs: structure and function. *Cells* **10**, 2825 (2021).
10. Bouchard, D. et al. SUMO paralogue–specific functions revealed through systematic analysis of human knockout cell lines and gene expression data. *Mol. Biol. Cell* **32**, 1849–1866 (2021).
11. Wang, W. & Matunis, M. J. Paralogue-specific roles of SUMO1 and SUMO2/3 in protein quality control and associated diseases. *Cells* **13**, 8 (2024).
12. Streich, F. C. Jr & Lima, C. D. Capturing a substrate in an activated RING E3/E2–SUMO complex. *Nature* **536**, 304–308 (2016).
13. Varejão, N. et al. Structural basis for the E3 ligase activity enhancement of yeast Nse2 by SUMO-interacting motifs. *Nat. Commun.* **12**, 7013 (2021).
14. Cappadocia, L., Pichler, A. & Lima, C. D. Structural basis for catalytic activation by the human ZNF451 SUMO E3 ligase. *Nat. Struct. Mol. Biol.* **22**, 968–975 (2015).
15. Eisenhardt, N. et al. A new vertebrate SUMO enzyme family reveals insights into SUMO-chain assembly. *Nat. Struct. Mol. Biol.* **22**, 959–967 (2015).
16. Hoppe, T. Multiubiquitylation by E4 enzymes: 'one size' doesn't fit all. *Trends Biochem. Sci.* **30**, 183–187 (2005).
17. Novatchkova, M., Bachmair, A., Eisenhaber, B. & Eisenhaber, F. Proteins with two SUMO-like domains in chromatin-associated complexes: the RENi (Rad60-Esc2-NIP45) family. *BMC Bioinforma.* **6**, 22 (2005).
18. Choi, K., Szakal, B., Chen, Y.-H., Branzei, D. & Zhao, X. The Smc5/6 complex and Esc2 influence multiple replication-associated recombination processes in *Saccharomyces cerevisiae*. *MBoC* **21**, 2306–2314 (2010).
19. Jørgensen, S. W. et al. Esc2 promotes telomere stability in response to DNA replication stress. *Nucleic Acids Res.* **47**, 4597–4611 (2019).
20. Sebesta, M. et al. Esc2 promotes Mus81 complex-activity via its SUMO-like and DNA binding domains. *Nucleic Acids Res.* **45**, 215–230 (2017).
21. Sollier, J. et al. The *Saccharomyces cerevisiae* Esc2 and Smc5-6 proteins promote sister chromatid junction-mediated intra-S repair. *MBoC* **20**, 1671–1682 (2009).

22. Prudden, J., Perry, J. J. P., Arvai, A. S., Tainer, J. A. & Boddy, M. N. Molecular mimicry of SUMO promotes DNA repair. *Nat. Struct. Mol. Biol.* **16**, 509–516 (2009).
23. Hertz, E. P. T. et al. The SUMO–NIP45 pathway processes toxic DNA catenanes to prevent mitotic failure. *Nat. Struct. Mol. Biol.* **30**, 1303–1313 (2023).
24. Li, S. et al. Esc2 orchestrates substrate-specific sumoylation by acting as a SUMO E2 cofactor in genome maintenance. *Genes Dev*. https://doi.org/10.1101/gad.344739.120 (2021).
25. Bergink, S. & Jentsch, S. Principles of ubiquitin and SUMO modifications in DNA repair. *Nature* **458**, 461–467 (2009).
26. Suhandynata, R. T. et al. Shared and distinct roles of Esc2 and Mms21 in suppressing genome rearrangements and regulating intracellular sumoylation. *PLoS ONE* **16**, e0247132 (2021).
27. Bermúdez-López, M. et al. Sgs1's roles in DNA end resection, HJ dissolution, and crossover suppression require a two-step SUMO regulation dependent on Smc5/6. *Genes Dev.* **30**, 1339–1356 (2016).
28. Bonner, J. N. et al. Smc5/6 mediated sumoylation of the Sgs1-Top3-Rmi1 complex promotes removal of recombination intermediates. *Cell Rep.* **16**, 368–378 (2016).
29. Li, S. et al. Multifaceted regulation of the sumoylation of the Sgs1 DNA helicase. *J. Biol. Chem.* **298**, 102092 (2022).
30. Hobbs, B., Drant, J. & Williamson, M. P. The measurement of binding affinities by NMR chemical shift perturbation. *J. Biomol. NMR* **76**, 153–163 (2022).
31. Williamson, M. P. Using chemical shift perturbation to characterise ligand binding. *Prog. Nucl. Magn. Reson. Spectrosc.* **73**, 1–16 (2013).
32. Williamson, M. P. Chemical shift perturbation. In *Modern Magnetic Resonance* 1–19 https://doi.org/10.1007/978-3-319-28275-6-76-1 (Springer, Cham, 2017).
33. Sekiyama, N. et al. Structural basis for regulation of poly-SUMO chain by a SUMO-like domain of Nip45. *Proteins: Struct. Funct. Bioinforma.* **78**, 1491–1502 (2010).
34. Duda, D. M. et al. Structure of a SUMO-binding-motif mimic bound to Smt3p–Ubc9p: conservation of a non-covalent ubiquitin-like protein–E2 complex as a platform for selective interactions within a SUMO pathway. *J. Mol. Biol.* **369**, 619–630 (2007).
35. Knipscheer, P., van Dijk, W. J., Olsen, J. V., Mann, M. & Sixma, T. K. Noncovalent interaction between Ubc9 and SUMO promotes SUMO chain formation. *EMBO J.* **26**, 2797–2807 (2007).
36. Yunus, A. A. & Lima, C. D. Structure of the Siz/PIAS SUMO E3 ligase Siz1 and determinants required for SUMO modification of PCNA. *Mol. Cell* **35**, 669–682 (2009).
37. Psakhye, I. & Jentsch, S. Protein group modification and synergy in the SUMO pathway as exemplified in DNA repair. *Cell* **151**, 807–820 (2012).
38. Ohya, T., Arai, H., Kubota, Y., Shinagawa, H. & Hishida, T. A SUMO-like domain protein, Esc2, is required for genome integrity and sister chromatid cohesion in *Saccharomyces cerevisiae*. *Genetics* **180**, 41–50 (2008).
39. Urulangodi, M. et al. Local regulation of the Srs2 helicase by the SUMO-like domain protein Esc2 promotes recombination at sites of stalled replication. *Genes Dev.* **29**, 2067–2080 (2015).
40. Albuquerque, C. P. et al. Distinct SUMO ligases cooperate with Esc2 and Slx5 to suppress duplication-mediated genome rearrangements. *PLoS Genet.* **9**, e1003670 (2013).
41. Cho, T., Hoeg, L., Setiaputra, D. & Durocher, D. NFATC2IP is a mediator of SUMO-dependent genome integrity. *Genes Dev.* **38**, 233–252 (2024).
42. Varejão, N. et al. DNA activates the Nse2/Mms21 SUMO E3 ligase in the Smc5/6 complex. *EMBO J.* **37**, e98306 (2018).

Acknowledgements

We thank the Biomolecular NMR Facility at the University of Sheffield for providing instrumentation and technical support.

Author contributions

H.B.-G., M.M., and N.V. conducted all protein expression and in vitro activity assays. R.doA.M. and M.P.W. conducted the NMR experiments. R.S.-S. and J.T.-R. conducted all yeast in vivo assays. D.R., N.V., and J.T.-R. contributed to the correction and writing of the manuscript.

Funding

This work was supported by the Spanish Ministry of Science and Innovation (MICINN) PID2024-160233OB-I00 to D.R., and by ICREA to D.R., ICREA-Academia-2022, from Generalitat de Catalunya. DR acknowledges support from the Serra Hunter program from Generalitat de Catalunya. The work in J.T.-R. lab was supported by grants PID2021-127689NB-I00 and PID2024-161654NB-I00 from MICIN/AEI/10.13039/501100011033/ and European Union Regional Funds (FEDER). The IRBLLEIDA institute is part of the CERCA. R.S.-S. was supported by a junior post-doctoral contract from Universitat de Lleida. The BBSRC (UK) for funding an upgrade to the NMR spectrometer (grant BB/R000727/1).

Competing interests

The authors declare no competing interests.

Additional information

Supplementary information The online version contains supplementary material available at https://doi.org/10.1038/s42003-026-10806-8.

Correspondence and requests for materials should be addressed to Nathalia Varejão or David Reverter.

Peer review information *Communications Biology* thanks the anonymous reviewers for their contribution to the peer review of this work. Primary handling editors: Elah Pick and Eve Rogers. A peer review file is available.